

Cbfb2 isoform dominates more potent Cbfb1 and is required for skeletal development

Qing Jiang¹, Xin Qin¹, Tetsuya Kawane¹, Hisato Komori¹, Yuki Matsuo¹, Ichiro Taniuchi², Kosei Ito³, Shin-ichi Izumi¹, and Toshihisa Komori¹ *

¹Department of Cell Biology and ³Department of Molecular Bone Biology, Nagasaki University Graduate School of Biomedical Sciences, 1-7-1, Nagasaki 852-8588, Japan

²Laboratory for Transcriptional Regulation, RIKEN Research Center for Allergy and Immunology, Yokohama, Japan.

*Corresponding author: Toshihisa Komori,

Department of Cell Biology, Nagasaki University Graduate School of Biomedical Sciences, 1-7-1, Nagasaki 852-8588, Japan

Tel: +81-95-819-7630

Fax: +81-95-819-7630

E-mail address: komorit@nagasaki-u.ac.jp

Abstract

Cbfb is a co-transcription factor that forms a heterodimer with Runx proteins, Runx1, Runx2, and Runx3. It is required for fetal liver hematopoiesis and skeletal development. Cbfb has two functional isoforms, Cbfb1 and Cbfb2, which are formed by alternative splicing. To address the biological functions of these isoforms in skeletal development, we examined *Cbfb1*^{-/-} and *Cbfb2*^{-/-} mouse embryos. Intramembranous and endochondral ossification was retarded and chondrocyte and osteoblast differentiation was inhibited in *Cbfb2*^{-/-} embryos but not in *Cbfb1*^{-/-} embryos. *Cbfb2* mRNA was upregulated in calvariae, limbs, livers, thymuses, and hearts of *Cbfb1*^{-/-} embryos but *Cbfb1* mRNA was not in those of *Cbfb2*^{-/-} embryos, and the total amount of *Cbfb1* and *Cbfb2* mRNA in *Cbfb1*^{-/-} embryos was similar to that in wild-type embryos, but was severely reduced in *Cbfb2*^{-/-} embryos. The absolute numbers of *Cbfb2* mRNA in calvariae, limbs, livers, thymuses, and brains in wild-type embryos were about three times higher than those of *Cbfb1* in the respective tissue. The levels of Runx proteins were reduced in calvariae, limbs, and primary osteoblasts from *Cbfb2*^{-/-} embryos, but the reduction in Runx2 protein was very mild. Furthermore, the amounts of Runx proteins and Cbfb in *Cbfb2*^{-/-} embryos differed similarly among skeletal tissues, livers, and thymuses, suggesting that Runx proteins and Cbfb are mutually required for their stability. Although *Cbfb1*^{-/-} embryos developed normally, Cbfb1 induced chondrocyte and osteoblast differentiation and enhanced DNA binding of Runx2 more efficiently than Cbfb2. Our results indicate that modulations in the relative levels of the isoforms may adjust transcriptional activation by Runx2 to appropriate physiological levels. Cbfb2 was more abundant, but Cbfb1 was more potent for enhancing Runx2 activity. While only Cbfb2 loss generated

overt skeletal phenotypes, both may play major roles in skeletal development with functional redundancy.

Keywords: Developmental modeling; Molecular pathways-development; Transcription factors; Osteoblasts; Growth plate

Introduction

Cbfb is a co-transcription factor that forms a heterodimer with Runx family transcription factors.⁽¹⁾ Cbfb has an α/β structure consisting of two three-stranded β -sheets packed on one another in a sandwich arrangement, with four peripheral α -helices.⁽²⁾ Inversion of chromosome 16 involves breakage of *CBFB*, and is associated with acute myeloid leukemia in humans. *Cbfb*^{-/-} mice die at midgestation due to the absence of fetal liver hematopoiesis, which is similar to the phenotype of *Runx1*^{-/-} mice, indicating that Runx1 and Cbfb are essential for hematopoietic stem cell differentiation. Cbfb is also required for skeletal development, which is shown by the partial rescue of the lack of fetal liver hematopoiesis in *Cbfb*^{-/-} mice or the insertion of GFP into exon 5 of *Cbfb*.⁽³⁻⁵⁾ The requirement for Cbfb in skeletal development is also shown by the deletion of *Cbfb* in mesenchymal cells.⁽⁶⁻¹¹⁾ Cbfb enhances the transcriptional activities of Runx family proteins by enhancing their DNA binding capacity and stabilizing Runx family proteins. In addition to the functions as a co-transcription factor for Runx family proteins, Cbfb is required for degradation of the retroviral complementary DNA deaminase APOBEC3G, which is a cellular protein that dominantly blocks virus replication and promotes HIV infection.⁽¹²⁾

The Runx family consists of Runx1, Runx2, and Runx3.⁽¹⁾ These transcription factors act as master regulators in different cell lineages with some overlapping functions. Runx1 is essential for hematopoietic stem cell differentiation and is involved in acute myeloid leukemia. Runx1 is also involved in chondrocyte differentiation, at least, in the development of some of the endochondral bones. Runx3 plays important roles in the growth regulation of gastric epithelial cells, neurogenesis, and activation of natural killer cells, and is related to many cancers. Runx1 and Runx3 are required for

thymocyte development, and Runx3 has a redundant function with Runx2 in chondrocyte maturation. Runx3 is also involved in the proliferation of osteoblast lineage cells.⁽¹³⁾ Runx2 is an essential transcription factor for osteoblast differentiation and is required for chondrocyte maturation.^(14,15) Heterozygous mutation of *RUNX2* causes cleidocranial dysplasia (CCD), which is characterized by hypoplastic clavicles, open fontanelles, and supernumerary teeth, and *Runx2*^{+/-} mice also show hypoplastic clavicles and open fontanelles.⁽¹⁶⁾

Multiple Cbfb cDNA clones were isolated, and the two of their proteins, Cbfb p22.0 composed of 187 amino acids that is called here as Cbfb1 and Cbfb p21.5 composed of 182 amino acids that is called here as Cbfb2, form a complex with Runx family proteins.^(17,18) Cbfb1 and Cbfb2 are formed by alternative splicing using donor splice sites located inside exon 5 and at the 3' terminus of exon 5, respectively, and an acceptor splice site located at the 5' terminus of exon 6.⁽¹⁸⁾ Although Cbfb2 is required for the differentiation of lymphoid tissue inducer cells and the development of mucosa-associated lymphoid tissue,^(19,20) the functions of the two isoforms in skeletal development are completely unknown. In this study, we examined the skeletal development of mice lacking the Cbfb1 isoform (*Cbfb1*^{-/-}) and mice lacking the Cbfb2 isoform (*Cbfb2*^{-/-}). *Cbfb1*^{-/-} mice developed normally. However, *Cbfb2*^{-/-} mice showed dwarfism, and both endochondral ossification and intramembranous ossification were inhibited. Although Cbfb1 was more potent for enhancing Runx2 function, the formation of Cbfb1 isoform was strictly regulated in skeletal tissues, livers, and thymuses, in which Runx family transcription factors play important roles in osteoblast and chondrocyte differentiation, hematopoiesis, and T-cell development, respectively.

Materials and methods

Mice

Cbfb^{+/-}, *Cbfb1*^{-/-}, *Cbfb2*^{-/-}, and *Cbfb*^{fl/fl/Cre} mice were generated as previously described.^(10,19,21) In brief, with the splice signal for *Cbfb1* located inside of exon 5, the GTG was mutated to CTC, and with the splice signal for *Cbfb2* at the 3' terminus of exon 5, GTTAG was mutated to AATTC. *Cbfb*^{fl/fl/Cre} mice were generated by using *Cbfb*^{fl/fl} mice and *Dermo1* Cre knock-in mice, in which Cre is expressed in mesenchymal cells giving rise to both chondrocyte and osteoblast lineages. The backgrounds of these mice were a mixed 129Ola/C57BL6 background. Prior to the study, all experimental protocols were reviewed and approved by the Animal Care and Use Committee of Nagasaki University Graduate School of Biomedical Sciences (No. 1403111129-8). The animals were housed 4 per cage in pathogen-free environment on a 12 h light cycle at 22 ± 2 °C with standard chow (CLEA Japan, Tokyo) and had free access to tap water.

Skeletal and histological analyses

We stained whole skeletons at embryonic day (E) 15.5 with alcian blue and alizarin red, as described previously.⁽¹⁴⁾ For histological analysis, whole bodies of E16.5 embryos were fixed in 4% paraformaldehyde in 0.1 M phosphate buffer pH 7.4 overnight at 4 °C, immersed in 10% EDTA in PBS overnight at 4 °C, and embedded in paraffin. The blocks were sectioned at 5 µm in thickness and the sections were subjected to hematoxylin and eosin (H-E) staining and *in situ* hybridization. Von Kossa staining was performed as previously described.⁽¹⁴⁾

***In situ* hybridization**

For *in situ* hybridization, we prepared single-stranded RNA probes labeled with digoxigenin-11-dUTP using a DIG RNA Labeling Kit (Roche Biochemicals,

Switzerland) according to the manufacturer's instructions. We used a 0.4-kb fragment of mouse *Col2a1* cDNA,⁽²²⁾ a 0.65-kb fragment of mouse *Col10a1* cDNA,⁽²²⁾ and a 1.2-kb fragment of mouse *osteopontin* cDNA⁽²²⁾ to generate antisense and sense probes. We carried out *in situ* hybridization as described previously⁽¹⁴⁾ and the sections were counterstained with methyl green.

Real-time reverse-transcription polymerase chain reaction (RT-PCR) analysis

Total RNA was extracted using ISOGEN (Wako, Osaka, Japan), and real-time RT-PCR analyses were performed as previously described.⁽²³⁾ Primer sequences are shown in Table S1. We normalized the values to those of β -actin.

Western blot analysis

Western blot was performed using a newly generated mouse monoclonal anti-Cbfb antibody, rabbit polyclonal anti-Runx1 antibody,⁽¹⁰⁾ anti-Runx2 (Cell Signaling, Danvers, MA), anti-Runx3 (Cell Signaling), and anti- β -actin (Santa Cruz Biotechnology, Santa Cruz, CA) antibodies.

Micromass culture

Primary chondrocytes isolated from the limb skeletons of *Cbfb2*^{+/+}, *Cbfb1*^{-/-}, and *Cbfb2*^{-/-} embryos at E15.5 were cultured in DMEM/Nutrient Mixture F-12 Ham (Sigma) containing 5% FBS and 10 μ g/ml transferrin (Roche Diagnostics). A total of 1×10^5 cells in 10 μ l of medium were placed in a micromass in the center of a 24-well plate and cultured for 1 h, and then 0.5 ml of medium was added. To induce chondrocyte differentiation, 10 mM β -glycerophosphate and 50 μ g/ml ascorbic acid were added. To compare the functions of Cbfb1 and Cbfb2, primary chondrocytes from *Cbfb*^{fl/fl/Cre} mice were transfected with an expression vector, pcDNA3.1, inserted with enhanced green fluorescent protein (EGFP), *Cbfb1*, or *Cbfb2* by using Neon Transfection System

(Invitrogen), and micromass culture was performed.

In vitro osteoblastogenesis, reporter assay, and chromatin immunoprecipitation (ChIP) assay

Primary osteoblasts were isolated from calvariae at E18.5 as previously described.⁽¹⁴⁾ To examine osteoblast differentiation, staining for alkaline phosphatase (ALP) activity and mineralization was performed as previously described.⁽¹⁴⁾ To compare the functions of *Cbfb1* and *Cbfb2*, primary osteoblasts from *Cbfb^{fl/fl/Cre}* mice were transfected with an expression vector, pcDNA3.1, inserted with EGFP, *Cbfb1*, or *Cbfb2* by using the Neon Transfection System (Invitrogen). In reporter assay, primary osteoblasts from newborn calvariae were transfected with 1.3 kb *Bglap2* promoter construct and pRL-TK (Promega) using X-tremeGENE9 (Roche Diagnostics). ChIP assay was performed using anti-Runx2 (Santa Cruz Biotechnology) or anti-IgG (Cell signaling) antibody in primary osteoblasts from newborn calvariae as previously described.⁽²⁴⁾

Droplet digital PCR

The absolute quantity of mRNA was measured by the QX200 Droplet Digital PCR System (BIO-RAD) using EvaGreen application reagents (BIO-RAD). The absolute values of mRNA were normalized by those of β -actin mRNA.

Electrophoresis mobility shift assay (EMSA)

Runx2-I that is derived from proximal P2 promoter, Runx2-II that is derived from distal P1 promoter, *Cbfb1*, and *Cbfb2* were generated by *in vitro* transcription/translation using the T7 Coupled TNT Rabbit Reticulocyte Lysate System (Promega) according to the manufacturer's protocol. EMSA was performed as previously described.⁽²⁵⁾ OSE2 oligonucleotide sequences were as follows: 5'-

CCGCTGCAATCACCAACCACAGCATC-3', and the mutated oligonucleotide, 5'-CCGCTGCAATCACCAAGAACAGCATC-3'. Anti-Runx2 (Cell Signaling) and anti-Cbfb antibodies were used in supershift assays.

Statistical analysis

Values are shown as mean \pm SD. Statistical analyses of two groups were performed by Student's t-test, and those of more than three groups were performed by ANOVA and the Tukey-Kramer post hoc test. A p-value of less than 0.05 was considered significant.

Results

Cbfb2^{-/-} embryos but not Cbfb1^{-/-} embryos showed delayed mineralization

To assess the processes of intramembranous and endochondral ossification, the skeletal system was examined at E15.5. Mineralized tissues are stained red and cartilage is stained blue. The sizes of the skeletons were similar among wild-type, *Cbfb1^{-/-}*, and *Cbfb2^{+/-}* embryos, and the mineralization of skeletons was also similarly observed among them (Fig. 1a-c). However, the sizes of skeletons were smaller and the mineralization in calvaria, mandible, maxilla, vertebrae, ribs, and limbs was severely reduced in *Cbfb2^{-/-}* embryos compared with those in wild-type embryos (Fig. 1a, d). The embryos with heterozygous deletion of *Cbfb* (*Cbfb^{+/-}*) showed similar skeletal size but mild reduction in the mineralization in both intramembranous and endochondral bones compared with their wild-type (*Cbfb^{+/+}*) littermates (Fig. 1e, f).

The process of endochondral ossification was retarded in Cbfb2^{-/-} embryos but not in Cbfb1^{-/-} embryos

Histological analysis of femurs showed that bone marrow cavity and trabecular bone structure were formed in wild-type, *Cbfb1*^{-/-}, and *Cbfb2*^{+/-} embryos at E16.5, whereas they were not formed and vascular invasion to the calcified cartilage had just started at the mid-diaphyses in *Cbfb2*^{-/-} embryos (Fig. 2A-H). *In situ* hybridization showed that *Col2a1*, which is expressed in resting and proliferating chondrocytes, was expressed in the epiphysis and metaphysis of femurs in wild-type, *Cbfb1*^{-/-}, *Cbfb2*^{+/-}, and *Cbfb2*^{-/-} embryos, although the *Col2a1*-negative region was short in *Cbfb2*^{-/-} embryos (Fig. 2I-L). *Col10a1*, which is expressed in hypertrophic chondrocytes, was detected in the metaphysis of all of the embryos, although the distance between *Col10a1*-positive layers was short in *Cbfb2*^{-/-} embryos (Fig. 2M-P). *Spp1*, which is expressed in terminal hypertrophic chondrocytes and osteoblasts, was detected in the diaphysis in all of the embryos, although it was restricted to the mid-diaphysis in *Cbfb2*^{-/-} embryos (Fig. 2Q-T).

Real-time RT-PCR analysis was performed using limb skeletons at E15.5, when the whole limb skeletons were cartilaginous (Fig. 3A). The expression of *Cbfb1* was absent in *Cbfb1*^{-/-} embryos, similar in *Cbfb2*^{+/+} and *Cbfb2*^{+/-} embryos, and mildly reduced in *Cbfb2*^{-/-} embryos compared with that in *Cbfb2*^{+/+} embryos. The expression of *Cbfb2* was upregulated in *Cbfb1*^{-/-} embryos compared with that in *Cbfb2*^{+/+} embryos, reduced in *Cbfb2*^{+/-} embryos, and absent in *Cbfb2*^{-/-} embryos. The total amount of *Cbfb1* and *Cbfb2* mRNA was similar between *Cbfb2*^{+/+} and *Cbfb1*^{-/-} embryos, mildly reduced in *Cbfb2*^{+/-} embryos, and severely reduced in *Cbfb2*^{-/-} embryos compared with that in *Cbfb2*^{+/+} embryos. The expression of *Sox9*, *Sox5*, and *Sox6* was upregulated in *Cbfb2*^{-/-} embryos but not in *Cbfb1*^{-/-} embryos and *Cbfb2*^{+/-} embryos compared with that in *Cbfb2*^{+/+} embryos. The expression of *Col2a1*, *Acan*, *Ihh*, *Col10a1*, *Runx1*, and *Runx3* was similar among *Cbfb2*^{+/+}, *Cbfb1*^{-/-}, *Cbfb2*^{+/-}, and *Cbfb2*^{-/-} embryos, while *Spp1* expression

was severely reduced in *Cbfb2*^{-/-} embryos and *Runx2* expression was upregulated in *Cbfb2*^{-/-} embryos compared with those in *Cbfb2*^{+/+} embryos. Upregulation of *Runx2* expression is likely to be due to negative autoregulation.⁽⁵⁾ The protein levels of Runx1, Runx2, Runx3, and Cbfb in *Cbfb2*^{-/-} embryos were 30%, 90%, 60%, and 16% of those in *Cbfb2*^{+/+} embryos, respectively (Fig. 3B, C).

The expression of *Cbfb1* and *Cbfb2* and the total amount of *Cbfb1* and *Cbfb2* mRNA in *Cbfb*^{+/-} embryos were nearly half of those in *Cbfb*^{+/+} embryos; the expression levels of chondrocyte marker genes and Runx family genes in *Cbfb*^{+/-} embryos were similar to those in *Cbfb*^{+/+} embryos; and the protein levels of Runx1, Runx2, Runx3, and Cbfb in *Cbfb*^{+/-} embryos were 35%, 91%, 66%, and 67% of those in *Cbfb*^{+/+} embryos, respectively (Supplementary Fig. 1).

Osteoblast differentiation in calvariae was delayed in *Cbfb2*^{-/-} embryos but not in *Cbfb1*^{-/-} embryos

Real-time RT-PCR analysis was performed using RNA from calvarial tissues at E18.5 to examine osteoblast differentiation (Fig. 4A). *Cbfb1* mRNA was absent in *Cbfb1*^{-/-} calvariae and it was similar between *Cbfb2*^{+/+} and *Cbfb2*^{-/-} calvariae. *Cbfb2* mRNA was upregulated in *Cbfb1*^{-/-} calvariae and absent in *Cbfb2*^{-/-} calvariae. The total amounts of *Cbfb1* and *Cbfb2* mRNA were similar between *Cbfb2*^{+/+} and *Cbfb1*^{-/-} embryos and severely reduced in *Cbfb2*^{-/-} embryos compared with that in *Cbfb2*^{+/+} embryos. *Spp1* was significantly reduced in *Cbfb2*^{-/-} but not in *Cbfb1*^{-/-} calvariae compared with that in *Cbfb2*^{+/+} calvariae. The mRNA levels of *Runx1*, *Runx2*, and *Runx3* were similar among *Cbfb2*^{+/+}, *Cbfb1*^{-/-}, and *Cbfb2*^{-/-} calvariae. The protein level of Runx1 in *Cbfb2*^{-/-} calvariae was similar to that in *Cbfb2*^{+/+} calvariae at E18.5.

However, the protein levels of Runx2 and Runx3 in *Cbfb2*^{-/-} calvariae were 81% and 25% of those in *Cbfb2*^{+/+} calvariae, respectively (Fig. 4A-C). The protein level of Runx1 in *Cbfb2*^{-/-} calvariae was also examined at E15.5, and it was 18% of that in *Cbfb2*^{+/+} calvariae (Fig. 4D, E). As hematopoietic cells had been more abundantly observed in calvarial region at E18.5 than E15.5 in histological analysis (data not shown), we examined Runx1 protein in peripheral blood from newborn mice. The levels of Runx1 protein were similar between *Cbfb2*^{+/+} and *Cbfb2*^{-/-} mice (Fig. 4D, E). Further, the similar tendencies with the data at E18.5 in the mRNA levels of osteoblast marker genes and Runx family genes and in the protein levels of Runx2, Runx3, and Cbfb were observed at E15.5 (Supplementary figure 2). Therefore, the data at E15.5 was more likely to reflect the Runx1 protein levels in osteoblasts and their progenitors. The protein level of Cbfb in *Cbfb2*^{-/-} calvariae was 28% of that in *Cbfb2*^{+/+} calvariae (Fig. 4B, C).

In *Cbfb*^{+/-} calvariae, the expression of *Cbfb1* and *Cbfb2* and the total amount of *Cbfb1* and *Cbfb2* mRNA were nearly half of those in *Cbfb*^{+/+} calvariae, the expression of *Colla1* was mildly reduced, and the expression of the other osteoblast marker genes and Runx family genes was similar to that in *Cbfb*^{+/+} calvariae. The protein levels of Runx1, Runx2, Runx3, and Cbfb in *Cbfb*^{+/-} calvariae were 30%, 98%, 47%, and 37% of those in *Cbfb*^{+/+} calvariae, respectively (Supplementary Fig. 3).

Chondrocyte differentiation was inhibited in Cbfb2^{-/-} *chondrocytes but not in Cbfb1*^{-/-} *chondrocytes*

To examine chondrocyte differentiation, micro-mass culture was performed. After culture for 10 days, primary chondrocytes from *Cbfb2*^{+/+} and *Cbfb1*^{-/-} embryos were

similarly stained by alcian blue, but the staining was reduced in primary chondrocytes from *Cbfb2*^{-/-} embryos (Fig. 5A, B). In *Cbfb1*^{-/-} chondrocytes at day 10 and day 15, *Cbfb1* mRNA was absent, *Cbfb2* mRNA was upregulated, and the total amount of *Cbfb1* and *Cbfb2* mRNA was similar to that in *Cbfb1*^{+/+} chondrocytes (Fig. 5C). The expressions of the marker genes for chondrogenesis, *Col2a1* and *Acan*, and the marker genes for chondrocyte maturation, *Ihh*, *Col10a1*, and *Ibsp*, in *Cbfb1*^{-/-} chondrocytes were comparable to those in *Cbfb1*^{+/+} chondrocytes at day 10 and day 15 (Fig. 5C). The expressions of *Runx1*, *Runx2*, and *Runx3* were similar between *Cbfb1*^{+/+} and *Cbfb1*^{-/-} chondrocytes at day 10 and day 15.

In *Cbfb2*^{-/-} chondrocytes at day 10 and day 15, the levels of *Cbfb1* mRNA were similar to those in *Cbfb2*^{+/+} chondrocytes, *Cbfb2* mRNA was absent, and the total amount of *Cbfb1* and *Cbfb2* mRNA was reduced in *Cbfb2*^{-/-} chondrocytes compared with *Cbfb2*^{+/+} chondrocytes (Fig. 5D). The expression of *Ihh*, *Col10a1*, and *Runx2* was reduced at day 10, and the expression of *Acan* and *Ibsp* was reduced at day 15 (Fig. 5D).

Osteoblast differentiation was inhibited in *Cbfb2*^{-/-} osteoblasts but not in *Cbfb1*^{-/-} osteoblasts

Calvaria-derived primary osteoblasts were cultured in vitro. The levels of staining for ALP activity and mineralization were similar between *Cbfb1*^{+/+} and *Cbfb1*^{-/-} osteoblasts (Fig. 6A, B). In *Cbfb1*^{-/-} osteoblasts, *Cbfb1* was absent, *Cbfb2* was increased at day 5, and the total amount of *Cbfb1* and *Cbfb2* mRNA was similar to that in *Cbfb1*^{+/+} osteoblasts at day 5 and day 15. The expression levels of osteoblast marker genes, including *Alpl*, *Sp7*, *Colla1*, *Spp1*, *Bglap2*, and *Runx* family genes, were not significantly different from those in *Cbfb1*^{+/+} osteoblasts at day 5 and day 15 (Fig. 6D).

The protein levels of Runx1, Runx2, Runx3, and Cbfb in *Cbfb1*^{-/-} osteoblasts were similar to those in *Cbfb1*^{+/+} osteoblasts (Fig. 6F).

In *Cbfb2*^{-/-} osteoblasts, the levels of staining for ALP activity and mineralization were reduced compared with those in *Cbfb2*^{+/+} osteoblasts (Fig. 6A, C). The expression of *Cbfb1* was similar to that in *Cbfb2*^{+/+} osteoblasts at day 5 and mildly reduced at day 15, *Cbfb2* was absent, and the total amount of *Cbfb1* and *Cbfb2* mRNA was severely reduced compared with that in *Cbfb2*^{+/+} osteoblasts at day 5 and day 15 (Fig. 6E). The expression of *Alpl*, *Sp7*, *Colla1*, and *Bglap2* was reduced in *Cbfb2*^{-/-} osteoblasts at day 5 and day 15, and *Spp1* expression was reduced at day 15 compared with the respective level in *Cbfb2*^{+/+} osteoblasts. The expression of Runx family genes did not differ significantly between *Cbfb2*^{+/+} and *Cbfb2*^{-/-} osteoblasts. The proteins of Runx1, Runx3, and Cbfb were apparently reduced in *Cbfb2*^{-/-} osteoblasts compared with those in *Cbfb2*^{+/+} osteoblasts (Fig. 6F).

In the reporter assay using *Bglap2* promoter, the reporter activities were similar between *Cbfb1*^{+/+} and *Cbfb1*^{-/-} osteoblasts, whereas it was reduced in *Cbfb2*^{-/-} osteoblasts compared with that in *Cbfb2*^{+/+} osteoblasts (Fig. 6G, H). In ChIP assay, the level of the binding of Runx2 to the *Bglap2* promoter region in *Cbfb1*^{-/-} osteoblasts was similar to that in *Cbfb2*^{+/+} osteoblasts, but it was reduced in *Cbfb2*^{-/-} osteoblasts compared with those in *Cbfb2*^{+/+} and *Cbfb1*^{-/-} primary osteoblasts (Fig. 6I).

Expression of Cbfb1 was strictly regulated, Cbfb2 mRNA was about three times higher than Cbfb1 mRNA, and the amounts of Runx family proteins and Cbfb in Cbfb2^{-/-} embryos differed among tissues

Cbfb2 was upregulated in limbs and calvariae in *Cbfb1*^{-/-} embryos and primary

chondrocytes and osteoblasts from *Cbfb1*^{-/-} embryos, whereas *Cbfb1* was not upregulated in limbs and calvariae in *Cbfb2*^{-/-} embryos and primary chondrocytes and osteoblasts from *Cbfb2*^{-/-} embryos (Fig. 3A, 4A, 5C, 5D, 6D, 6E). Therefore, the expression of *Cbfb1* and *Cbfb2* was also examined in livers, thymuses, spleens, and hearts of *Cbfb2*^{+/+}, *Cbfb1*^{-/-}, and *Cbfb2*^{-/-} embryos at E15.5 (Fig. 7A). The expression of *Cbfb1* was similar or mildly reduced in *Cbfb2*^{-/-} embryos compared with that in *Cbfb2*^{+/+} embryos in all of the tissues, while *Cbfb2* was upregulated in *Cbfb1*^{-/-} embryos compared with that in *Cbfb2*^{+/+} embryos in all of the tissues. Therefore, the amount of *Cbfb1* mRNA was strictly regulated and compensatory upregulation of *Cbfb1* never occurred in the absence of *Cbfb2*, whereas compensatory upregulation of *Cbfb2* occurred in the absence of *Cbfb1* in all of the tissues. To compare the absolute numbers of *Cbfb1* and *Cbfb2* transcripts, droplet digital RT-PCR was performed (Fig. 7B). The numbers of *Cbfb2* mRNA were approximately three times higher than those of *Cbfb1* mRNA in calvariae, limbs, livers, thymuses, and brains of wild-type embryos. The total amounts of *Cbfb1* and *Cbfb2* were high in calvariae and limbs among these tissues.

Runx1 is essential for fetal liver hematopoiesis, and Runx1 and Runx3 have critical functions in lineage specification and homeostasis of CD8-lineage T lymphocytes.^(26,27) Therefore, Runx family proteins in livers and thymuses in *Cbfb2*^{+/+}, *Cbfb1*^{-/-}, and *Cbfb2*^{-/-} embryos at E15.5 were examined (Fig. 7C). The protein levels of Runx1, Runx2, Runx3, and Cbfb in both livers and thymuses of *Cbfb1*^{-/-} embryos were similar to the respective protein levels of *Cbfb2*^{+/+} embryos. The protein level of Runx2 in livers of *Cbfb2*^{-/-} embryos was similar to that of *Cbfb2*^{+/+} embryos, while the protein levels of Runx1, Runx3, and Cbfb in livers of *Cbfb2*^{-/-} embryos were mildly reduced compared with those of *Cbfb2*^{+/+} embryos. In thymuses, however, all of the protein

levels in *Cbfb2*^{-/-} embryos were reduced compared with those in *Cbfb2*^{+/+} embryos, and the protein levels of Runx1, Runx3, and Cbfb were extremely low.

Cbfb1 was more potent than Cbfb2 in chondrocyte and osteoblast differentiation and in enhancing DNA binding capacity of Runx2

To compare the individual functions of Cbfb1 and Cbfb2 in chondrocyte differentiation, EGFP, *Cbfb1*, or *Cbfb2* expression vector was introduced into primary chondrocytes from *Cbfb*^{fl/fl/Cre} embryos (Fig. 8A-C). As a control, EGFP was also introduced into primary chondrocytes from *Cbfb*^{fl/fl} embryos. Although similar amounts of *Cbfb1* and *Cbfb2* mRNA were expressed in *Cbfb*^{fl/fl/Cre} chondrocytes, the staining by alcian blue was stronger in *Cbfb1*-introduced cells than in *Cbfb2*-introduced ones.

Similarly, EGFP, *Cbfb1*, or *Cbfb2* was introduced into primary osteoblasts from *Cbfb*^{fl/fl/Cre} embryos (Fig. 8D-F). Although similar amounts of *Cbfb1* and *Cbfb2* mRNA were expressed in *Cbfb*^{fl/fl/Cre} primary osteoblasts, the induction of *Runx2*, *Alpl*, and *Bglap2* expression was stronger in *Cbfb1*-introduced cells than in *Cbfb2*-introduced ones, and ALP activity was also stronger in *Cbfb1*-introduced cells than in *Cbfb2*-introduced ones.

The abilities of Cbfb1 and Cbfb2 to enhance the DNA binding of Runx2 were compared by EMSA (Fig. 9). Neither Cbfb1 nor Cbfb2 alone had the ability to bind DNA. However, both enhanced DNA binding of Runx2-I and Runx2-II. Cbfb1 was more potent than Cbfb2 in enhancing the DNA binding of Runx2-I and Runx2-II.

Discussion

Cbfb2^{-/-} embryos but not *Cbfb1*^{-/-} embryos showed delays in the processes of both endochondral and intramembranous ossification. The differentiation of *Cbfb2*^{-/-} chondrocytes and osteoblasts was inhibited, whereas that of *Cbfb1*^{-/-} chondrocytes and osteoblasts was normal. One of the reasons for the differential phenotypes in the isoform-specific knockout mice was the expression levels of the two isoforms. The expression level of *Cbfb2* was about three times higher than that of *Cbfb1* in calvaria and limb skeletal tissues. In *Cbfb1*^{-/-} skeletal tissues and in the isolated chondrocytes and osteoblasts, *Cbfb2* mRNA was always increased compared with that in wild-type embryos. In *Cbfb2*^{-/-} skeletal tissues and in the isolated chondrocytes and osteoblasts, however, *Cbfb1* mRNA was never increased and the levels were similar to those of wild-type embryos. Therefore, the total amount of *Cbfb1* and *Cbfb2* mRNA in *Cbfb1*^{-/-} embryos was similar to that in wild-type embryos, whereas that in *Cbfb2*^{-/-} embryos was severely reduced. Therefore, the regulation of alternative splicing was responsible for the differential phenotypes in the isoform-specific knockout mice.

The ratios of *Cbfb1* mRNA and *Cbfb2* mRNA were similar among the tissues examined, and *Cbfb2* mRNA was three times more abundant than *Cbfb1* mRNA. *Cbfb2* mRNA was increased not only in skeletal tissues but also in livers, thymuses, spleens, and hearts in *Cbfb1*^{-/-} embryos, but *Cbfb1* mRNA was not increased in all of these tissues in *Cbfb2*^{-/-} embryos. These findings suggest that the alternative splicing for *Cbfb1* is strictly regulated, and that the differential expression levels of the two isoforms in wild-type mice were due to the restricted splicing for the *Cbfb1* isoform. In the formation of *Cbfb1* isoform mRNA, a donor splice site located inside of exon 5 is used. Specific serine-arginine-rich (SR) proteins bind to exon splicing enhancer (ESE) elements, which are located in the exon or adjacent intron sequence, and activate splicing by interacting

with components of the spliceosome to stabilize their binding to adjacent splice sites.⁽²⁸⁾ ESEs also play an important role in alternative splicing.⁽²⁹⁾ There are 11 ESE candidates for SR proteins, including Srsf1, Srsf2, Srsf5, and Srsf6, in exon 5 and the adjacent intron sequence of *Cbfb*. We transfected the expression vectors of *Srsf1*, *Srsf2*, *Srsf4*, *Srsf5*, or *Srsf6* into wild-type, *Cbfb1*^{-/-}, and *Cbfb2*^{-/-} primary osteoblasts. However, neither *Cbfb1* nor *Cbfb2* mRNA was increased in these cells (data not shown). Phosphorylation of SR proteins is probably required or SR proteins are not sufficient for the activation of splicing.⁽²⁸⁾ As *Cbfb1* was more potent than *Cbfb2* in the induction of chondrocyte and osteoblast differentiation, and in the enhancement of DNA binding of Runx2, strict regulation of the alternative splicing for *Cbfb1* mRNA may be important for the regulation of skeletal development. It will be interesting to compare the functions of *Cbfb1* and *Cbfb2* in hematopoiesis, neurogenesis, T-cell development, activation of natural killer cells, and oncogenesis.

Cbfb stabilizes Runx family proteins.^(10,11) The total amount of *Cbfb1* and *Cbfb2* mRNA in *Cbfb1*^{-/-} osteoblasts was similar to that of wild-type osteoblasts, and the protein levels of Runx1, Runx2, and Runx3 in *Cbfb1*^{-/-} osteoblasts were similar to those in wild-type osteoblasts. These findings indicate that *Cbfb1* and *Cbfb2* had similar abilities to stabilize Runx family proteins. This was also true in livers and thymuses. In *Cbfb2*^{-/-} osteoblasts, the total amount of *Cbfb1* and *Cbfb2* mRNA was severely reduced and the protein levels of Runx1, Runx2, and Runx3 were also reduced, indicating that the stability of Runx family proteins was dependent on the total amount of *Cbfb1* and *Cbfb2*. This is also true in *Cbfb*^{+/-} limbs and calvariae, in which the amounts of *Cbfb1* and *Cbfb2* mRNA were nearly half of those in wild-type limbs and calvariae and the Runx1 and Runx3 proteins were reduced. However, the dependence of Runx family proteins on

Cbfb1 and Cbfb2 in terms of their stability differed. Runx2 was nearly stable in a state of insufficiency of Cbfb1, Cbfb2, or both in skeletal tissues and livers. Runx2 protein is probably protected not only by Cbfb but also by other proteins, but insufficiency of Cbfb reduces the DNA binding of Runx2.

The stability of Runx family proteins in a state of insufficiency of Cbfb also differed among skeletal tissues, livers, and thymuses: Runx2 was stable in skeletal tissues and livers and moderately unstable in thymuses; Runx1 and Runx3 were moderately unstable in skeletal tissues and livers and extremely unstable in thymuses. These findings may indicate that the proteins that can substitute for Cbfb in the stabilization of Runx family proteins differ in each Runx protein, and that the abundance of these proteins differs among the tissues. Indeed, it is also possible that the proteins that substitute for Cbfb are common among Runx family proteins and they stabilize Runx family proteins at differing efficiencies among them. Interestingly, the protein levels of Cbfb also differed among skeletal tissues, livers, and thymuses in *Cbfb2*^{-/-} embryos. The levels of *Cbfb* mRNA in these tissues of *Cbfb2*^{-/-} embryos were about one fourth of that of wild-type embryos. However, the amounts of Cbfb protein were about half in livers, one sixth in skeletal tissues, and less than one tenth in thymuses in *Cbfb2*^{-/-} embryos compared with the respective amount in those of wild-type embryos. As the reduction of Cbfb protein was parallel to that of Runx family proteins in these tissues of *Cbfb2*^{-/-} embryos, these findings may indicate that the stability of Cbfb is also dependent on the amounts of Runx family proteins.

Our findings indicate that Cbfb isoforms had two different functions in the regulation of Runx family proteins. One was stabilization of Runx family proteins, in which Cbfb1 and Cbfb2 had similar activities. The other was enhancement of the DNA

binding of Runx2, in which Cbfb1 was more potent than Cbfb2. However, the core structure domain of Cbfb for heterodimerization with Runt domain is located to N-terminal 141 amino acids, which are included in both Cbfb1 and Cbfb2.^(2,30) Therefore, the drugs for modulating Runx/Cbfb interaction may not be able to show differing effects on Cbfb1 and Cbfb2. It needs to be resolved how Cbfb1 had more ability to enhance DNA binding of Runx2 than Cbfb2. Further, as Cbfb1 had more ability to enhance osteoblast and chondrocyte differentiation than Cbfb2, these isoforms may have different abilities to interact with transcription factors, cofactors including TLE/groucho proteins, and histone modifying proteins. Finally, the strict conservation of the ratio of *Cbfb1* and *Cbfb2* mRNA in various tissues may be important for maintaining the activity of Runx family proteins at appropriate physiological levels during skeletal development, hematopoiesis, and T-cell development.

Disclosures

All of the authors state that they have no conflicts of interest.

Acknowledgments

We thank Dr. D Ornitz for *Dermo1* Cre knock-in mice. This work was supported by the grant from the Japanese Ministry of Education, Culture, Sports, Science and Technology to TK (Grant number: 26221310).

Authors' roles: Study design: TK. Data acquisition: QJ, XQ, TK, HK, YM, KI, and SI. Data analysis and interpretation: QJ, XQ, TK, HK, IT, and TK. Drafting manuscript: TK. Approving final version of manuscript: QJ, XQ, TK, HK, YM, IT, KI, SI, and TK. TK takes responsibility for the integrity of the data analysis.

References

1. Komori T. Regulation of skeletal development by the Runx family of transcription factors. *J Cell Biochem.* 2005;95(3):445-53.
2. Huang X, Peng JW, Speck NA, Bushweller JH. Solution structure of core binding factor beta and map of the CBF alpha binding site. *Nat Struct Biol.* 1999;6(7):624-7.
3. Kundu M, Javed A, Jeon JP, et al. Cbfbeta interacts with Runx2 and has a critical role in bone development. *Nat Genet.* 2002;32(4):639-44.
4. Miller J, Horner A, Stacy T, et al. The core-binding factor beta subunit is required for bone formation and hematopoietic maturation. *Nat Genet.* 2002;32(4):645-9.
5. Yoshida CA, Furuichi T, Fujita T, et al. Core-binding factor beta interacts with Runx2 and is required for skeletal development. *Nat Genet.* 2002;32(4):633-8.
6. Fei T, Mengrui W, Lianfu D, et al. Core binding factor beta (Cbf β) controls the balance of chondrocyte proliferation and differentiation by upregulating Indian hedgehog (Ihh) expression and inhibiting parathyroid hormone-related protein receptor (PPR) expression in postnatal cartilage and bone formation. *J Bone Miner Res.* 2014;29(7):1564-74.
7. Chen W, Ma J, Zhu G, et al. Cbfbeta deletion in mice recapitulates cleidocranial dysplasia and reveals multiple functions of Cbfbeta required for skeletal development. *Proc Natl Acad Sci U S A.* 2014;111(23):8482-7.
8. Wu M, Li C, Zhu G, et al. Deletion of core-binding factor beta (Cbfbeta) in mesenchymal progenitor cells provides new insights into Cbfbeta/Runxs complex function in cartilage and bone development. *Bone.* 2014;65:49-59.
9. Wu M, Li YP, Zhu G, et al. Chondrocyte-specific Knockout of Cbfbeta Reveals the Indispensable Function of Cbfbeta in Chondrocyte Maturation, Growth Plate Development and Trabecular Bone Formation in Mice. *Int J Biol Sci.* 2014;10(8):861-72.
10. Qin X, Jiang Q, Matsuo Y, et al. Cbfb regulates bone development by stabilizing Runx family proteins. *J Bone Miner Res.* 2015;30(4):706-14.
11. Lim KE, Park NR, Che X, et al. Core binding factor beta of osteoblasts maintains cortical bone mass via stabilization of Runx2 in mice. *J Bone Miner Res.* 2015;30(4):715-22.
12. Zhang W, Du J, Evans SL, Yu Y, Yu XF. T-cell differentiation factor CBF-beta regulates HIV-1 Vif-mediated evasion of host restriction. *Nature.* 2012;481(7381):376-9.
13. Bauer O, Sharir A, Kimura A, Hantisteanu S, Takeda S, Groner Y. Loss of osteoblast Runx3 produces severe congenital osteopenia. *Mol Cell Biol.* 2015;35(7):1097-109.
14. Komori T, Yagi H, Nomura S, et al. Targeted disruption of Cbfa1 results in a complete lack of bone formation owing to maturational arrest of osteoblasts. *Cell.* 1997;89(5):755-64.
15. Otto F, Thornell AP, Crompton T, et al. Cbfa1, a candidate gene for cleidocranial dysplasia syndrome, is essential for osteoblast differentiation and bone development. *Cell.* 1997;89(5):765-71.

16. Mundlos S, Otto F, Mundlos C, et al. Mutations involving the transcription factor CBFA1 cause cleidocranial dysplasia. *Cell*. 1997;89(5):773-9.
17. Wang S, Wang Q, Crute BE, Melnikova IN, Keller SR, Speck NA. Cloning and characterization of subunits of the T-cell receptor and murine leukemia virus enhancer core-binding factor. *Mol Cell Biol*. 1993;13(6):3324-39.
18. Ogawa E, Inuzuka M, Maruyama M, et al. Molecular cloning and characterization of PEBP2 beta, the heterodimeric partner of a novel Drosophila runt-related DNA binding protein PEBP2 alpha. *Virology*. 1993;194(1):314-31.
19. Tachibana M, Tenno M, Tezuka C, Sugiyama M, Yoshida H, Taniuchi I. Runx1/Cbfbeta2 complexes are required for lymphoid tissue inducer cell differentiation at two developmental stages. *J Immunol*. 2011;186(3):1450-7.
20. Nagatake T, Fukuyama S, Sato S, et al. Central Role of Core Binding Factor beta2 in Mucosa-Associated Lymphoid Tissue Organogenesis in Mouse. *PLoS One*. 2015;10(5):e0127460.
21. Sasaki K, Yagi H, Bronson RT, et al. Absence of fetal liver hematopoiesis in mice deficient in transcriptional coactivator core binding factor beta. *Proc Natl Acad Sci U S A*. 1996;93(22):12359-63.
22. Inada M, Yasui T, Nomura S, et al. Maturational disturbance of chondrocytes in Cbfa1-deficient mice. *Dev Dyn*. 1999;214(4):279-90.
23. Yoshida CA, Yamamoto H, Fujita T, et al. Runx2 and Runx3 are essential for chondrocyte maturation, and Runx2 regulates limb growth through induction of Indian hedgehog. *Genes Dev*. 2004;18(8):952-63.
24. Yoshida CA, Komori H, Maruyama Z, et al. SP7 Inhibits Osteoblast Differentiation at a Late Stage in Mice. *PLoS One*. 2012;7(3):e32364.
25. Kawane T, Komori H, Liu W, et al. Dlx5 and mef2 regulate a novel runx2 enhancer for osteoblast-specific expression. *J Bone Miner Res*. 2014;29(9):1960-9.
26. Okuda T, van Deursen J, Hiebert SW, Grosveld G, Downing JR. AML1, the target of multiple chromosomal translocations in human leukemia, is essential for normal fetal liver hematopoiesis. *Cell*. 1996;84(2):321-30.
27. Taniuchi I, Osato M, Egawa T, et al. Differential requirements for Runx proteins in CD4 repression and epigenetic silencing during T lymphocyte development. *Cell*. 2002;111(5):621-33.
28. Black DL. Mechanisms of alternative pre-messenger RNA splicing. *Annu Rev Biochem*. 2003;72:291-336.
29. Cartegni L, Wang J, Zhu Z, Zhang MQ, Krainer AR. ESEfinder: A web resource to identify exonic splicing enhancers. *Nucleic Acids Res*. 2003;31(13):3568-71.
30. Goger M, Gupta V, Kim WY, Shigesada K, Ito Y, Werner MH. Molecular insights into PEBP2/CBF beta-SMMHC associated acute leukemia revealed from the structure of PEBP2/CBF beta. *Nat Struct Biol*. 1999;6(7):620-3.

Figure legends

Fig. 1

Examination of skeletal system

(A) Whole skeletons of *Cbfb2*^{+/+}, *Cbfb1*^{-/-}, *Cbfb2*^{+/-}, *Cbfb2*^{-/-}, *Cbfb*^{+/+}, and *Cbfb*^{+/-} embryos at E15.5. *Cbfb2*^{+/+} wild-type embryo (a) is a littermate of *Cbfb2*^{+/-} (c) and *Cbfb2*^{-/-} (d) embryos. *Cbfb*^{+/+} wild-type embryo (e) is a littermate of *Cbfb*^{+/-} embryo (f). The skeletons of wild-type littermates of *Cbfb1*^{-/-} embryo (b), which were similar to those of *Cbfb2*^{+/+} embryo (a), are not shown. Skeletal size of *Cbfb2*^{-/-} embryos is apparently small (A-d). (B) Lateral view of the head. Mineralization of frontal and parietal bones, mandible, and maxilla was severely reduced in *Cbfb2*^{-/-} embryos (B-d). Mineralization of interparietal bone was delayed in *Cbfb*^{+/-} embryos compared with that in *Cbfb*^{+/+} embryos (B-e, f). (C) Bottom view of head. Mineralization of basioccipital, exoccipital, and sphenoid bones was nearly absent in *Cbfb2*^{-/-} embryos (C-d). These bones were less mineralized in *Cbfb*^{+/-} embryos than in *Cbfb*^{+/+} embryos (C-e, f). (D) Lateral view of chest wall. The mineralization of vertebrae was absent and that of ribs was severely reduced in *Cbfb2*^{-/-} embryos (D-d). The mineralization of vertebrae and ribs was mildly reduced in *Cbfb*^{+/-} embryos compared with that in *Cbfb*^{+/+} embryos (D-e, f). (E and F) Upper limbs (E) and lower limbs (F). The mineralization of limb bones and clavicle (arrow) was severely reduced in *Cbfb2*^{-/-} embryos (E-d, F-d). The mineralization of limb bones was mildly reduced in *Cbfb*^{+/-} embryos compared with that in *Cbfb*^{+/+} embryos (E-e, f; F-e, f). The mineralization in whole skeletons was similar among *Cbfb2*^{+/+}, *Cbfb1*^{-/-}, and *Cbfb2*^{+/-} embryos. Three embryos in each genotype were examined and representative data are shown. Scale bar: 1 mm.

Fig. 2

Histological analyses

H-E staining (A-D), von Kossa staining (E-H), in situ hybridization using *Col2a1* (I-L), *Col10a1* (M-P), and *Spp1* (Q-T) probes using sections of femurs in *Cbfb2*^{+/+} (A, E, I, M, Q), *Cbfb1*^{-/-} (B, F, J, N, R), *Cbfb2*^{+/-} (C, G, K, O, S), and *Cbfb2*^{-/-} (D, H, L, P, T) embryos at E16.5. The results of wild-type littermates of *Cbfb1*^{-/-} embryos, which were similar to those of *Cbfb2*^{+/+} embryos, are not shown. The boxed regions are magnified in the insets. *In situ* hybridization using the sense probes showed no significant signals (data not shown). Three embryos in each genotype were examined and representative data are shown. Scale bars: 0.5 mm.

Fig. 3

Real-time RT-PCR analysis of genes related to chondrocyte differentiation and Western blot analysis of Runx family proteins

(A) Real-time RT-PCR analysis. RNA was extracted from hind limb skeletons of *Cbfb2*^{+/+}, *Cbfb1*^{-/-}, *Cbfb2*^{+/-}, and *Cbfb2*^{-/-} embryos at E15.5. The values in *Cbfb2*^{+/+} embryos were defined as 1, and relative levels are shown. n=7-12. * vs. *Cbfb2*^{+/+} embryos. *p<0.05, **p<0.01. (B, C) Western blot analysis. Proteins were extracted from hind limb skeletons at E15.5. β -actin was used as an internal control. Representative data are shown in B. The intensities of bands were normalized against each β -actin, the normalized values in *Cbfb2*^{+/+} embryos were set as 1, and means of the relative levels are shown in C. The bands from 7-10 *Cbfb2*^{+/+} and *Cbfb2*^{-/-} embryos were quantitated.

Fig. 4

Real-time RT-PCR analysis of genes related to osteoblast differentiation and Western blot analysis of Runx family proteins

(A) Real-time RT-PCR analysis. RNA was extracted from calvariae of *Cbfb2*^{+/+}, *Cbfb1*^{-/-}, and *Cbfb2*^{-/-} embryos at E18.5. The values in *Cbfb2*^{+/+} embryos were defined as 1, and relative levels are shown. n=4-12. * vs. *Cbfb2*^{+/+} embryos. *p<0.05, **p<0.01. (B-E) Western blot analyses. Proteins were extracted from calvariae at E18.5 (B, C), and calvariae (Ca) at E15.5 and newborn (NB) peripheral blood (D, E). Representative data are shown in B and D. β -actin was used as an internal control. The intensities of bands were normalized against each β -actin, the normalized values in *Cbfb2*^{+/+} embryos were set as 1, and means of the relative levels are shown in C and E. The bands from 3-7 *Cbfb2*^{+/+} and *Cbfb2*^{-/-} embryos were quantitated.

Fig. 5

Micromass culture

Cbfb2^{+/+}, *Cbfb1*^{-/-}, and *Cbfb2*^{-/-} primary chondrocytes were plated in micromass (day 0), 10 mM β -glycerophosphate and 50 μ g/ml ascorbic acid were added to the medium at day 3, the cells were stained with alcian blue at day 10 (A), and the staining was quantitated by Image J (B). n=3. RNA was extracted for real-time RT-PCR at day 10 and day 15 (C, D). The values in wild-type chondrocytes at day 10 were defined as 1, and relative levels are shown. n=4. * vs. wild-type chondrocytes. *p<0.05, **p<0.01. Similar results were obtained in three independent experiments and representative data are shown.

Fig. 6

In vitro osteoblast differentiation, reporter assay, and ChIP assay

(A-C) ALP activity and mineralization. Primary osteoblasts from calvariae of *Cbfb1*^{+/+}, *Cbfb1*^{-/-}, *Cbfb2*^{+/+}, and *Cbfb2*^{-/-} embryos at E18.5 were subjected to ALP staining and von Kossa staining at 5 days and 30 days after confluence, respectively (A). The ALP staining and von Kossa staining were quantitated by Image J (B, C). n=3-4. (D, E) Real-time RT-PCR analysis. RNA was extracted at day 5 and day 15 after confluence (day 0). n=3-4. (F) Western blot analysis. Proteins were extracted at day 5. The intensities of the bands were normalized against each β -actin, the normalized values in *Cbfb1*^{+/+} or *Cbfb2*^{+/+} osteoblasts were set as 1, and relative levels are shown. (G, H) Reporter assay using *Bglap2* promoter. The luciferase activities in *Cbfb1*^{+/+} (G) or *Cbfb2*^{+/+} (H) osteoblasts transfected with pGL4 were set as 1, and relative activities are shown. n=4-6. (I) ChIP assay. DNA before immunoprecipitation (input) and after immunoprecipitation with anti-Runx2 or anti-IgG antibody was amplified by real-time PCR using primers that amplify the region containing the 189 bp of *Bglap2* promoter. The percentage against the input is shown. Similar results were obtained in two to four independent experiments and representative data are shown in A-I. * vs. *Cbfb1*^{+/+} or *Cbfb2*^{+/+} cells. *p<0.05, **p<0.01, ***p<0.001.

Fig. 7

The expression of *Cbfb1* and *Cbfb2* in various tissues

(A) Real-time RT-PCR analysis. RNA was extracted from livers, thymuses, spleens, and hearts in *Cbfb2*^{+/+}, *Cbfb1*^{-/-}, and *Cbfb2*^{-/-} embryos at E15.5, and the expression levels of *Cbfb1*, *Cbfb2*, and both *Cbfb1* and *Cbfb2* were examined. The values in

Cbfb2^{+/+} embryos were set as 1, and the relative levels are shown. n= 8-10. * vs. *Cbfb2*^{+/+} embryos. *p<0.05, **p<0.01. (B) Droplet digital RT-PCR. RNA was extracted from calvariae, limbs, livers, thymuses, and brains in wild-type embryos at E15.5, and the expression of *Cbfb1* and *Cbfb2* was examined. The value of *Cbfb1* in calvaria was set as 1, and the relative levels are shown. * vs. *Cbfb1*. ***p<0.001. n=3-4. (C) Western blot analysis. Proteins were extracted from livers and thymuses in *Cbfb2*^{+/+}, *Cbfb1*^{-/-}, and *Cbfb2*^{-/-} embryos at E15.5. β -actin was used as an internal control. The values in *Cbfb2*^{+/+} embryos were set as 1, and the relative levels are shown.

Fig. 8

Functional differences of *Cbfb1* and *Cbfb2*.

(A-C) Micromass culture of primary chondrocytes. Primary chondrocytes from *Cbfb*^{fl/fl} or *Cbfb*^{fl/fl/Cre} embryos at E15.5 were transfected with EGFP-, *Cbfb1*-, or *Cbfb2*-expression vector (day 0), RNA was extracted for real-time RT-PCR at day 3 (A), and alcian blue staining of *Cbfb*^{fl/fl/Cre} chondrocytes transfected with the indicated expression vectors was performed at day 21 (B) and quantitated by Image J (C). The values in *Cbfb*^{fl/fl} chondrocytes were set as 1, and the relative levels are shown in A. * vs. *Cbfb*^{fl/fl} chondrocytes. *p<0.05, **p<0.01. n=4. (D-F) In vitro osteoblastogenesis. Primary osteoblasts were prepared from calvariae in *Cbfb*^{fl/fl/Cre} embryos at E18.5, transfected with EGFP-, *Cbfb1*-, or *Cbfb2*-expression vector (day 0), RNA was extracted for real-time RT-PCR at day 3 (D), and ALP activity was examined at day 10 (E) and quantitated by Image J (F). The values in EGFP were set as 1, and the relative levels are shown. * vs. EGFP. *p<0.05, **p<0.01. n=4. Similar results were obtained in two independent experiments in A-F and representative data are shown.

Fig. 9

EMSA

EMSA was performed using OSE2 oligonucleotides that contain Runx2 binding motif, and proteins of EGFP, Runx2-I, Runx2-II, Cbfb1, and Cbfb2, which were generated by in vitro transcription/translation, as previously described.⁽²⁵⁾ (A) DNA binding of Runx2-I and Runx2-II without or with Cbfb1 or Cbfb2. (B) Competition with wild-type or mutated OSE2 oligonucleotides. wt, unlabeled wild-type OSE2 oligonucleotides (lanes 3, 9, 15, and 21, $\times 100$; lanes 4, 10, 16, and 22, $\times 25$; lanes 5, 11, 17, and 23, $\times 8$); mut, unlabeled mutated OSE2 oligonucleotides (lanes 6, 12, 18, and 24, $\times 100$). (C) Super-shifted complexes using antibody against Runx2 or Cbfb. Arrows indicate the specific bands and an arrowhead indicates the super-shifted complex. Addition of Cbfb antibody reduced the intensity of Runx2-Cbfb-DNA complex.

Supplementary Figure 1

Real-time RT-PCR analysis of genes related to chondrocyte differentiation and Western blot analysis of Runx family proteins in hind limb skeletons of *Cbfb*^{+/+} and *Cbfb*^{+/-} embryos at E15.5.

(A) Real-time RT-PCR analysis. The values in *Cbfb*^{+/+} embryos were defined as 1, and relative levels are shown. n=8-9. * vs. *Cbfb*^{+/+} embryos. ***p<0.001. (B) Western blot analysis. β -actin was used as an internal control. The intensities of the bands were normalized against each β -actin, the normalized values in *Cbfb*^{+/+} mice were set as 1, and relative levels are shown.

Supplementary Figure 2

Real-time RT-PCR analysis of genes related to osteoblast differentiation and Western blot analysis of Runx family proteins in calvariae of *Cbfb2*^{+/+}, *Cbfb1*^{-/-}, *Cbfb2*^{+/-}, and *Cbfb2*^{-/-} embryos at E15.5

(A) Real-time RT-PCR analysis. The values in *Cbfb2*^{+/+} embryos were defined as 1, and relative levels are shown. n=13-15. * vs. *Cbfb2*^{+/+} embryos. **p<0.01. (B) Western blot analysis. β -actin was used as an internal control. Representative data are shown. (C) The means of normalized values in *Cbfb2*^{+/+} embryos were set as 1, and means of the relative levels in *Cbfb2*^{-/-} embryos are shown. n=3-7. The representative band of Runx1 and mean of the relative levels are shown in Fig. 4D.

Supplementary Figure 3

Real-time RT-PCR analysis of genes related to osteoblast differentiation and Western blot analysis of Runx family proteins in calvariae of *Cbfb*^{+/+} and *Cbfb*^{+/-} embryos at E15.5.

(A) Real-time RT-PCR analysis. The values in *Cbfb*^{+/+} embryos were defined as 1, and relative levels are shown. n=9. * vs. *Cbfb*^{+/+} embryos. **p<0.01, ***p<0.001. (B) Western blot analysis. β -actin was used as an internal control. The intensities of the bands were normalized against each β -actin, the normalized values in *Cbfb*^{+/+} embryos were set as 1, and relative levels are shown.

Supplementary Table 1

Sequences of the oligonucleotides for real-time RT-PCR and ChIP.

Fig. 1

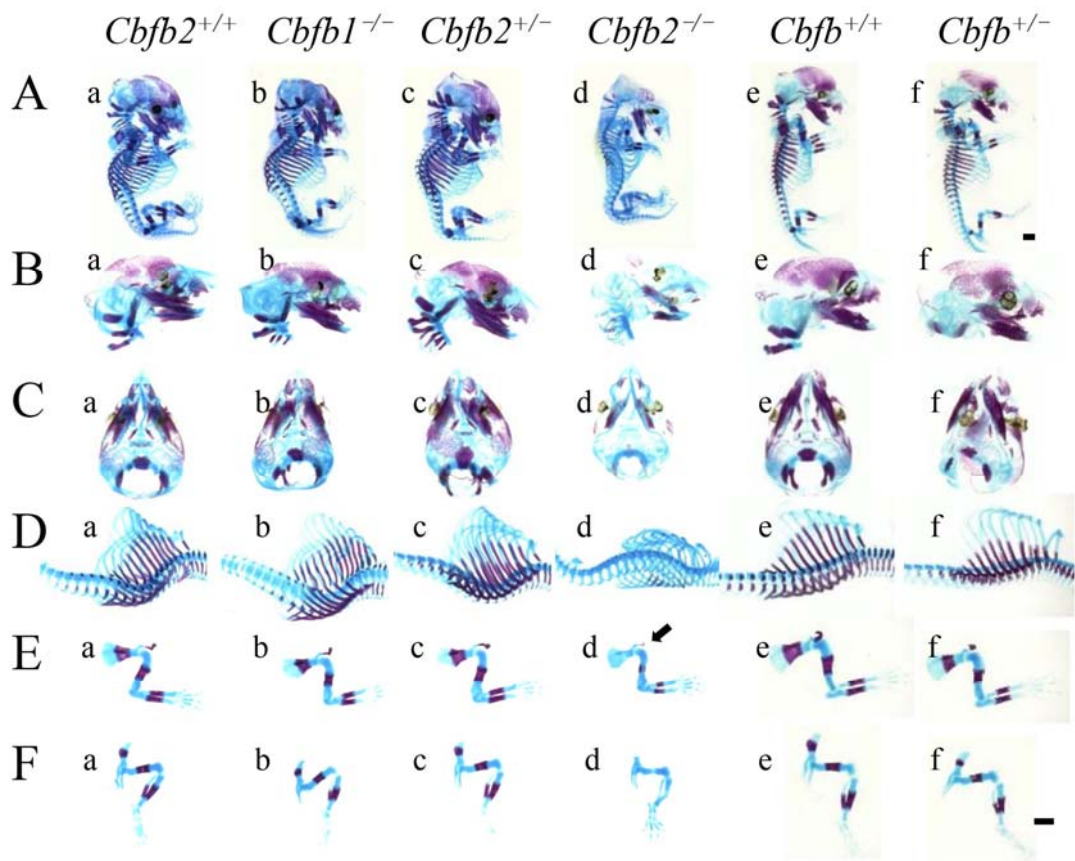


Fig. 2

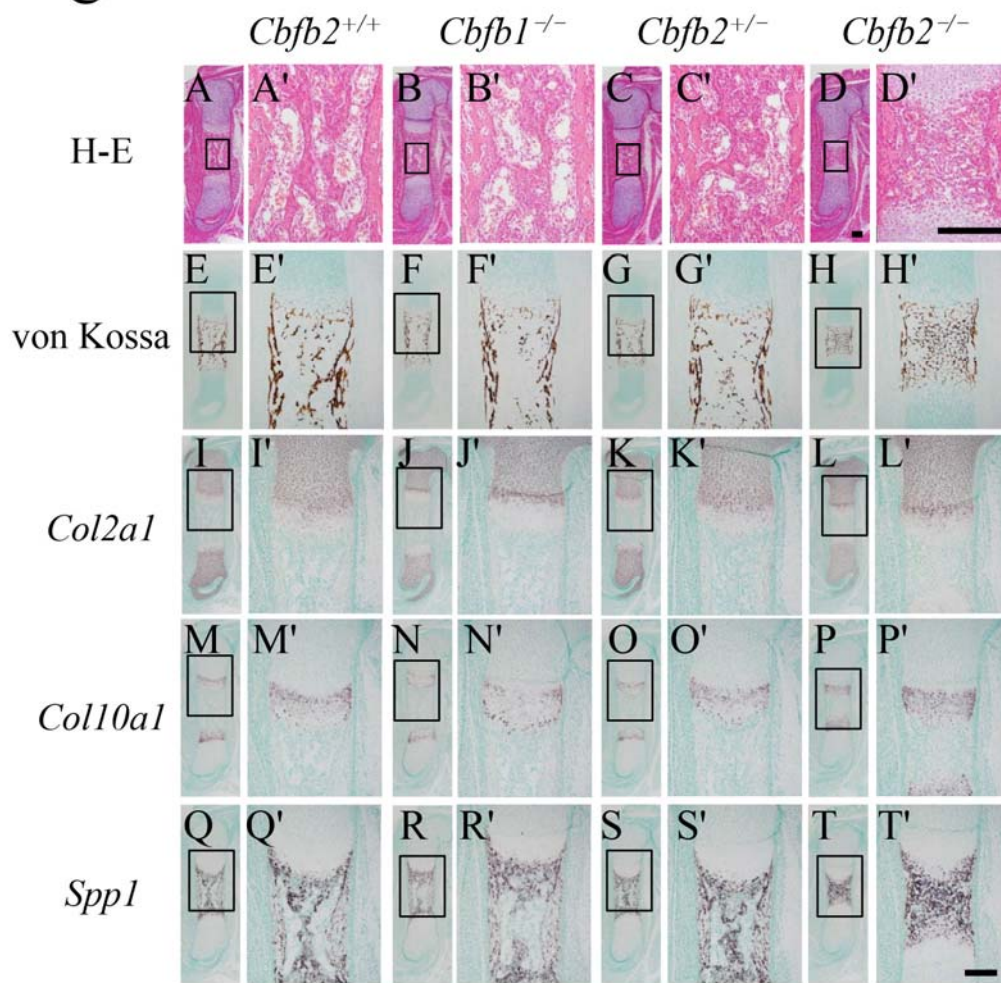


Fig. 3

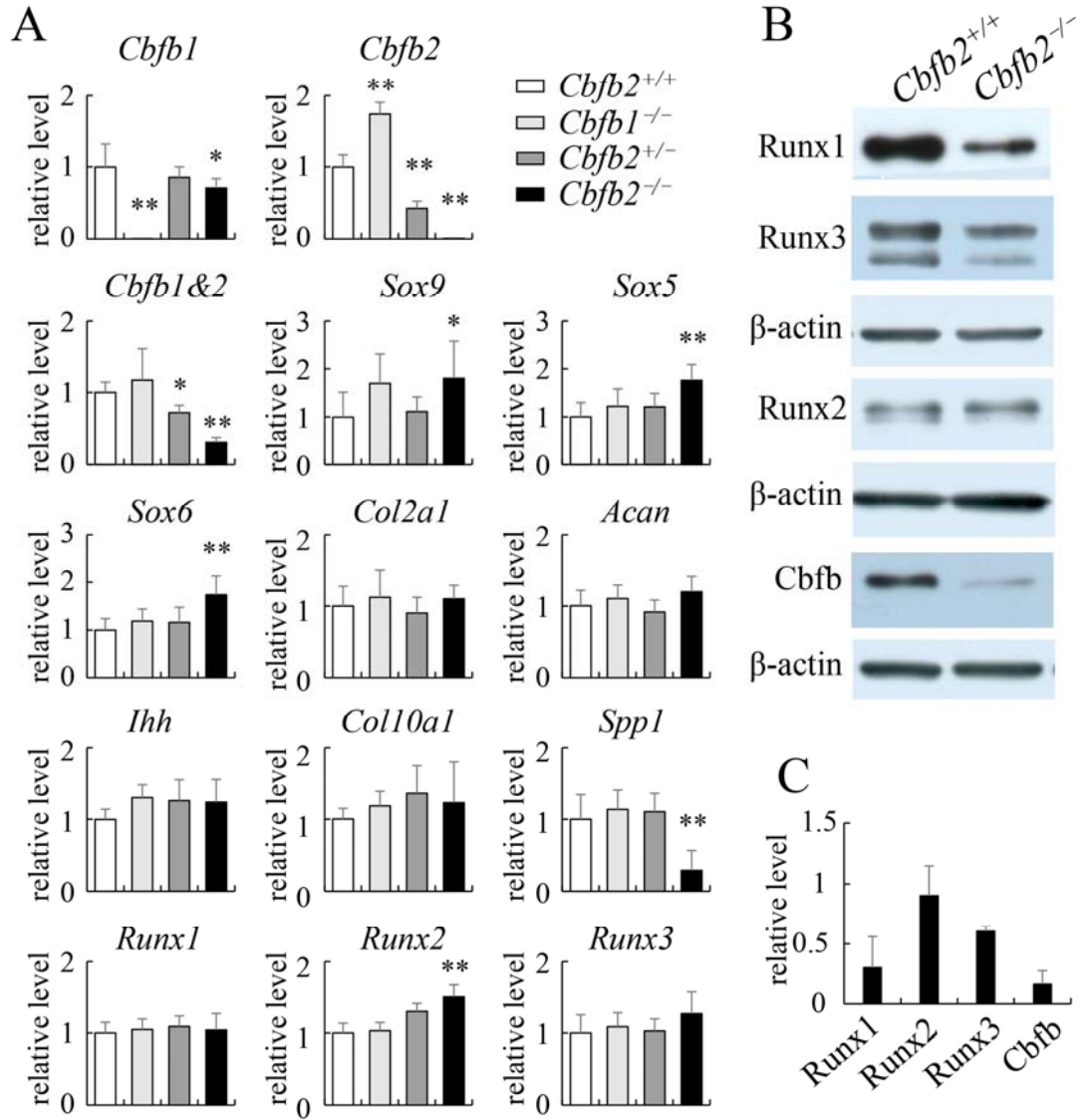


Fig. 4

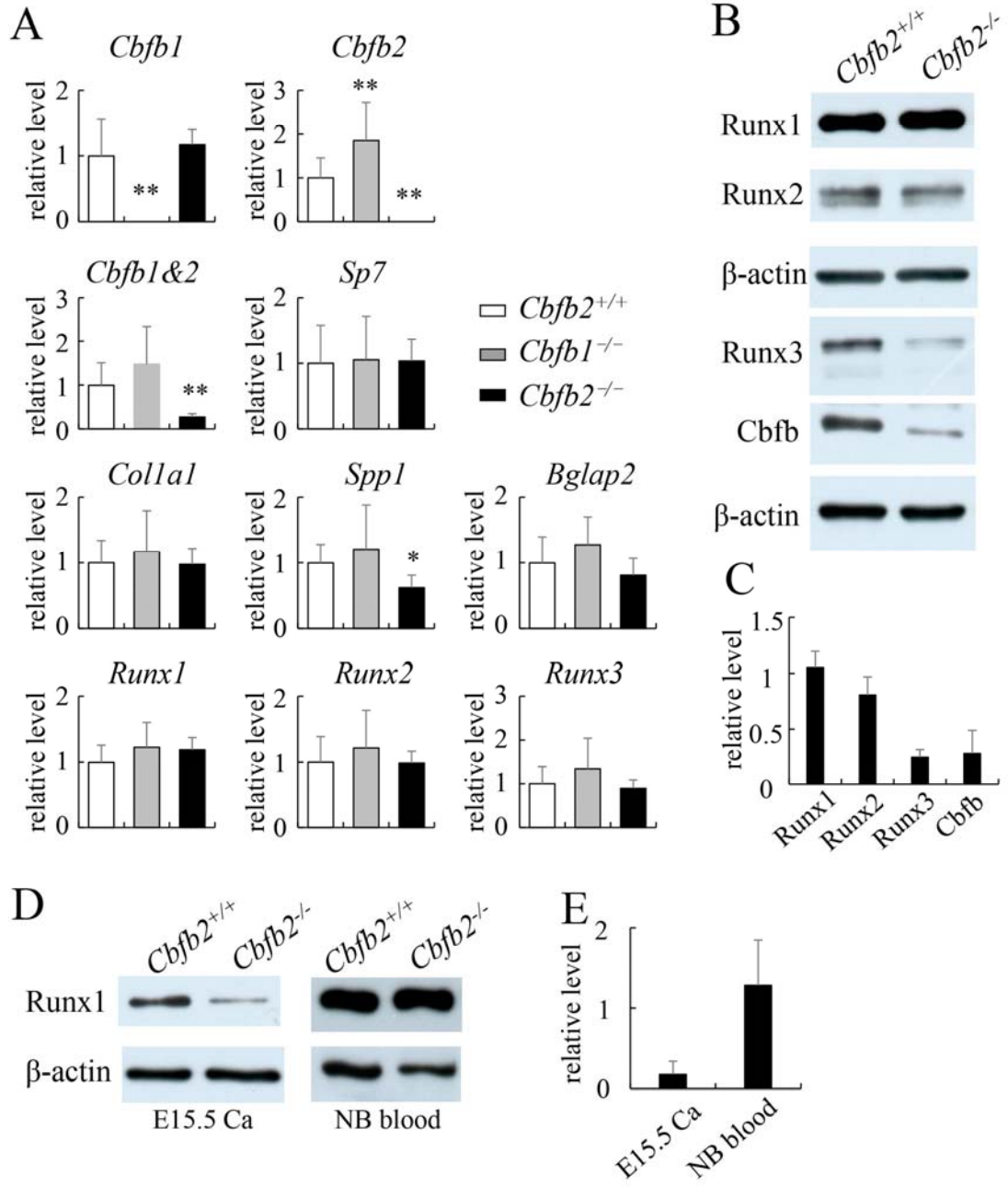


Fig. 5

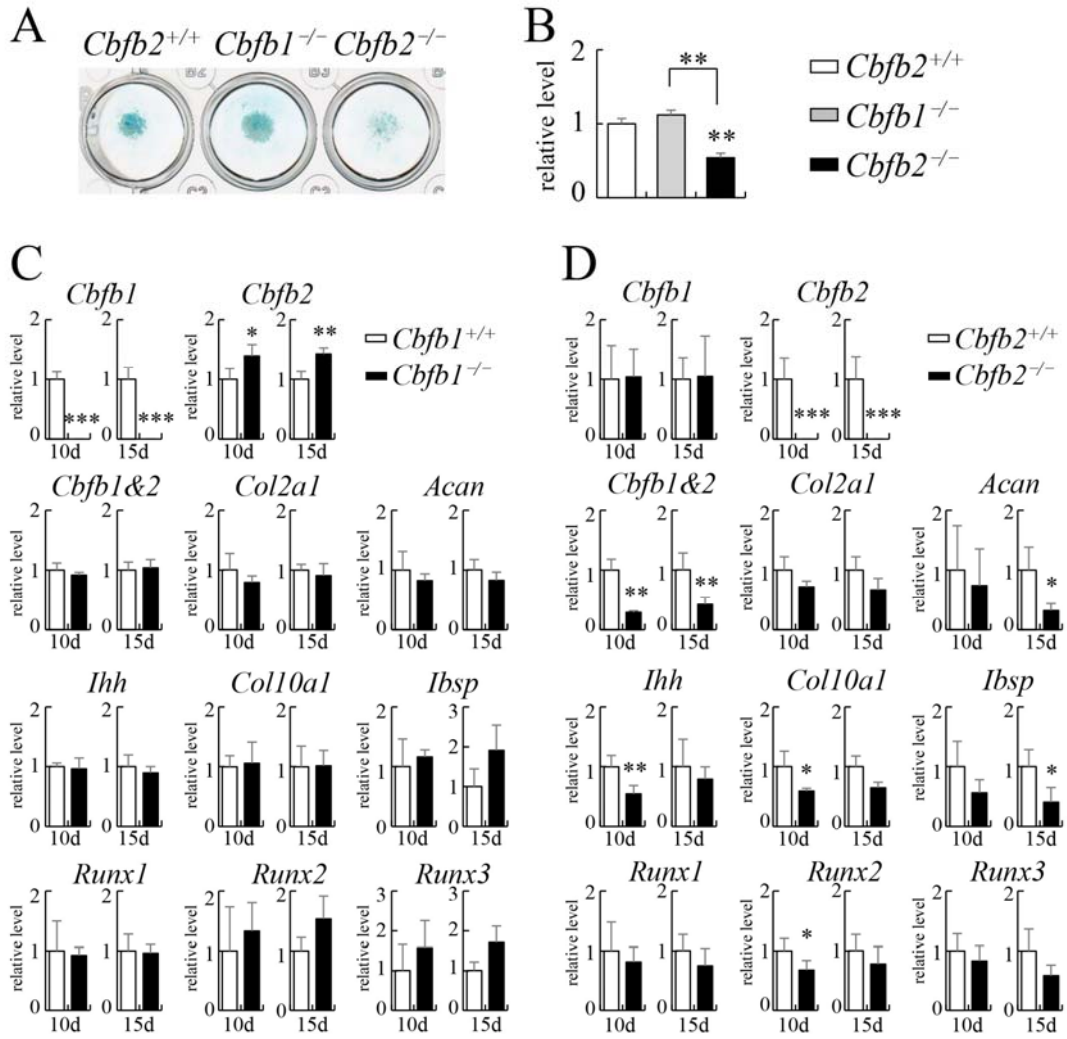


Fig. 6

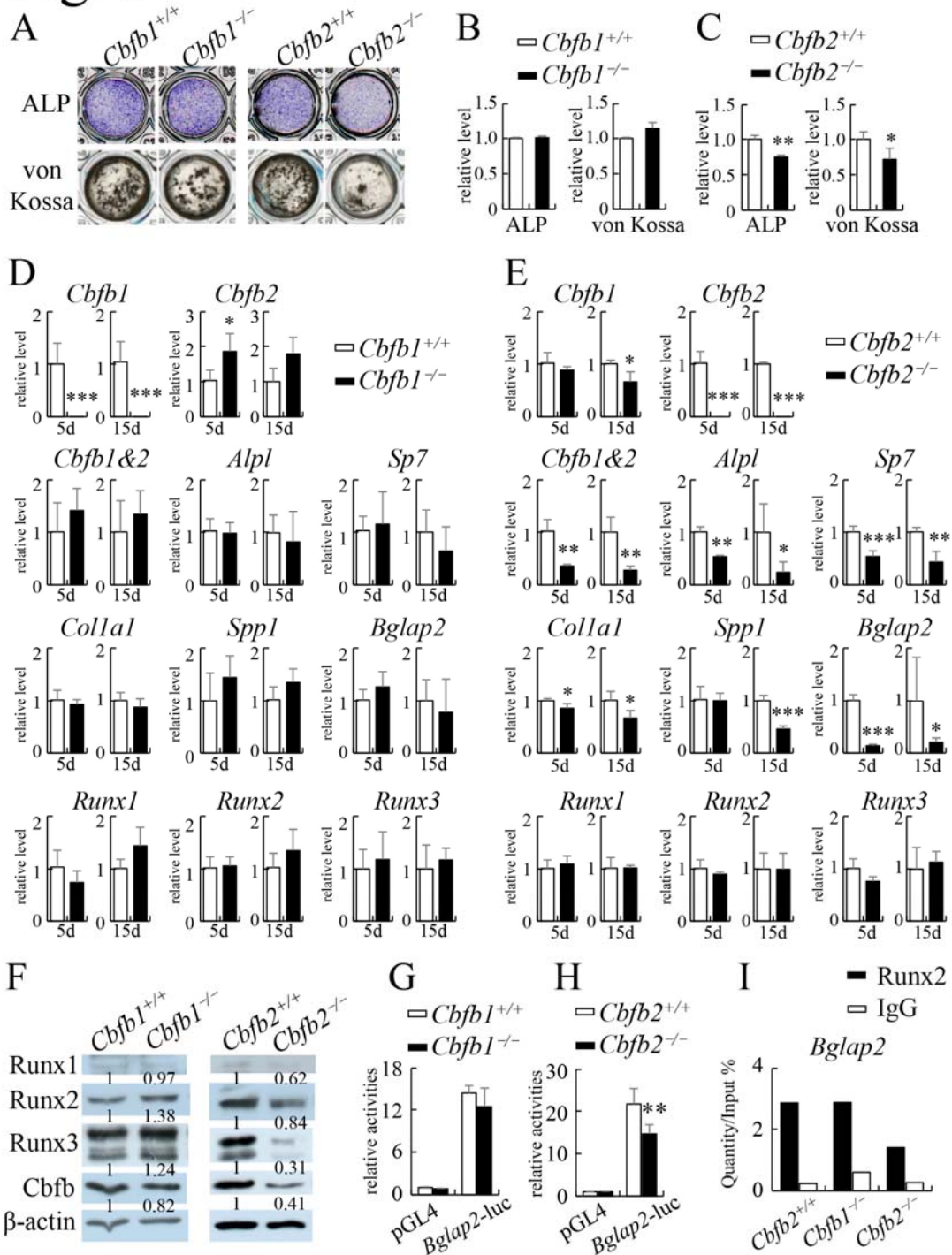
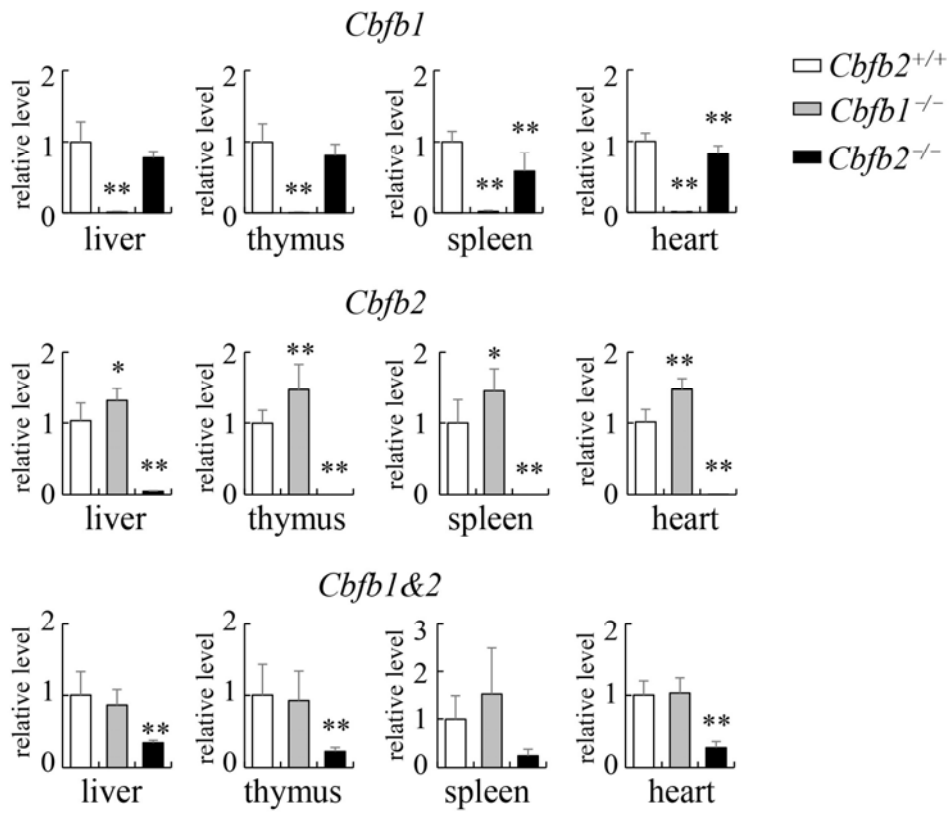
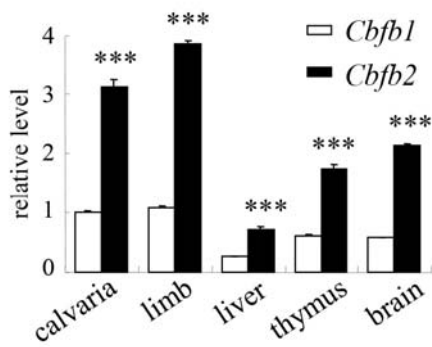


Fig. 7

A



B



C

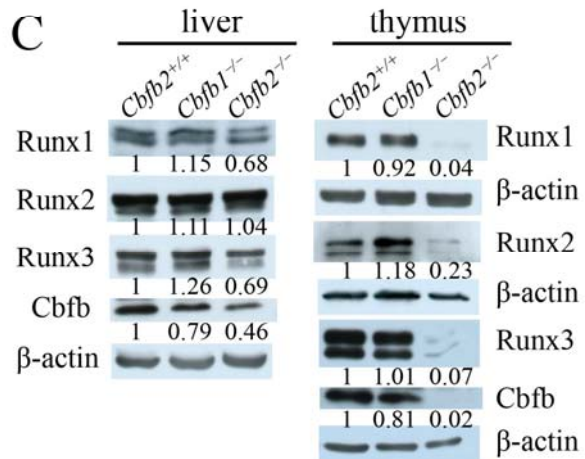


Fig. 8

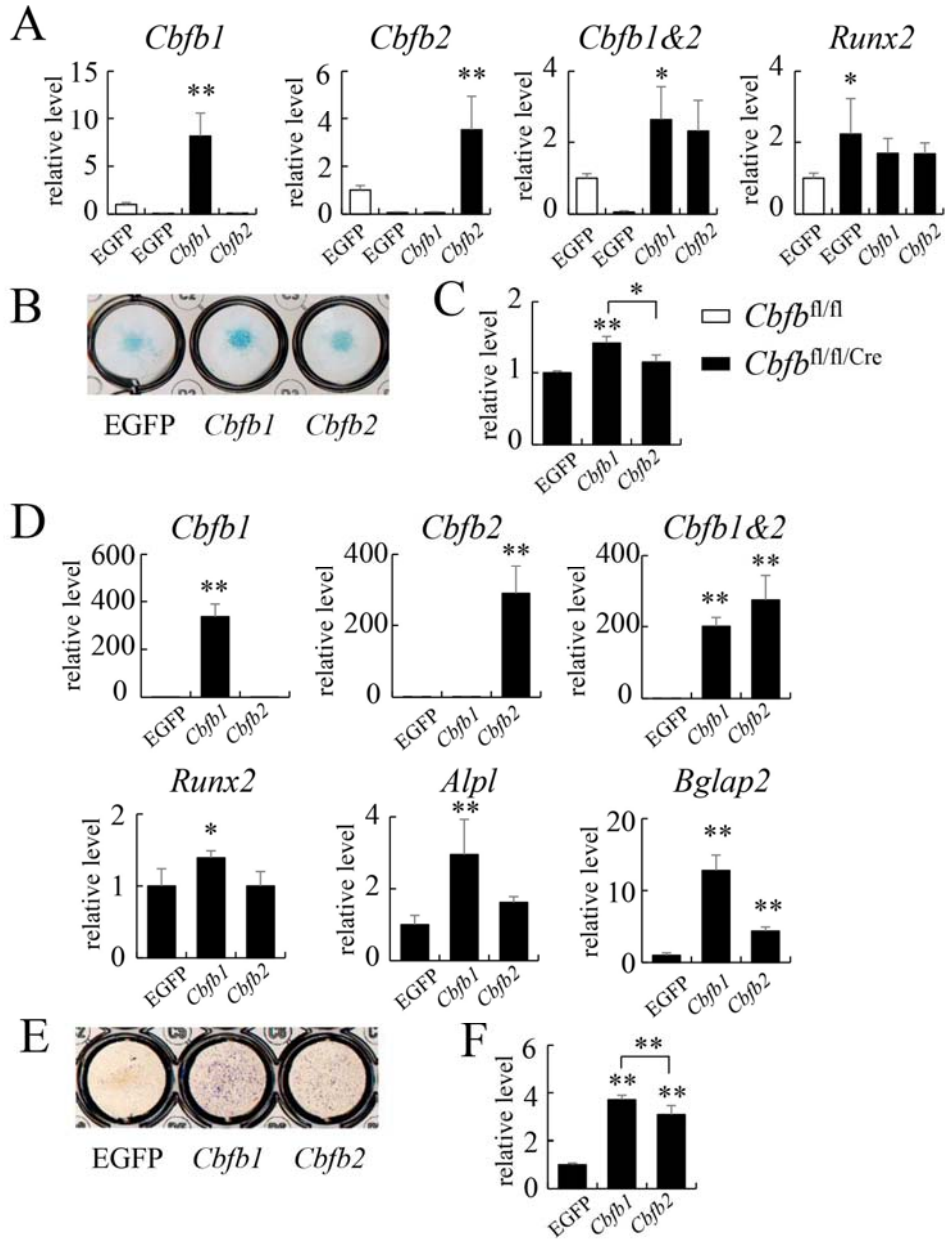


Fig. 9

